

Annual flux of dissolved organic carbon from the euphotic zone in the northwestern Sargasso Sea

Craig A. Carlson*, Hugh W. Ducklow†
& Anthony F. Michaels‡

* Horn Point Environmental Laboratory, University of Maryland,
PO Box 775, Cambridge, Maryland 21613, USA

† The College of William and Mary,
Virginia Institute of Marine Sciences, PO Box 1346,
Gloucester Point, Virginia 23062, USA

‡ Bermuda Biological Station for Research, Inc., St Georges GE-01,
Bermuda

THE export of biogenic carbon from the upper ocean is responsible for maintaining the vertical gradient of dissolved inorganic carbon and thus indirectly for regulating the level of atmospheric CO₂ (ref. 1). Large, rapidly sinking particles are thought to dominate this export², and this sinking flux has been thought to balance new production³. Recent measurements of particle export⁴⁻⁶ and estimates of new production⁷⁻⁹ have questioned this picture, however. Here we report measurements of dissolved organic carbon (DOC) off Bermuda, which provide strong support for the idea¹⁰⁻¹⁵ that this component of oceanic carbon is also an important and dynamic part of the ocean carbon cycle. We find that DOC accumulates in the early spring owing to increased primary production, and is partially consumed in the summer and autumn. The DOC that escapes remineralization is exported from the surface ocean the following winter, and we estimate this export to be equal to or greater than the measured particle flux, allowing us to close the annual vertical carbon budget for this site to within a factor of two. Our observations should be applicable to other temperate, sub-polar and continental-shelf regions of the world ocean which exhibit convective mixing and vernal restratification.

Renewed interest in DOC was sparked by a series of reports of elevated concentrations determined by the high-temperature combustion (HTC) method^{14,16} suggesting the presence of a previously unmeasured and chemically refractory pool. Although

these elevated DOC values have since proven to be incorrect¹⁷⁻²⁰, the controversy stimulated efforts to refine the HTC method, improving the precision and accuracy of the analysis of DOC in marine systems²⁰⁻²². Our average analytical precision is now <2% (comparable to ±1.1 μM C). This improved precision enables us to detect small changes in DOC concentrations and distributions and assess the role of DOC in global carbon cycling.

The samples were collected in the vicinity of the US JGOFS Bermuda Atlantic time-series study (BATS) station and Hydrostation S in the western Sargasso Sea. This site has strong seasonal patterns of mixing and biological production, dominated by a spring phytoplankton bloom^{5,6,23}. As in any oceanic system, mesoscale eddies may bias a discrete sample time series²⁴. We attempted to reduce the influence of mesoscale features on our sampling programme by making repeated measurements over periods of weeks within each season (except in autumn 1991 and winter 1992). This should allow our average seasonal profile to represent an integration of the mesoscale variability within each season (sampling programmes are detailed in Figs 1 and 2).

Vertical profiles show seasonal variability of DOC and temperature in the top 250 m (Fig. 1). The spring 1992 data were gathered during late bloom conditions. A broad subsurface DOC maximum developed between 40–60 m when the water column had completely restratified (Fig. 1a, b). By summer 1992 and 1993, a surface mixed layer of ~20 m developed, within which DOC concentrations were distributed homogeneously. Below this mixed layer a subsurface maximum persisted between 40–50 m (Fig. 1a). In the autumn of 1991 and 1992, the surface mixed layer deepened to ~50 and 60 m respectively (Fig. 1b) and DOC was distributed homogeneously within the mixed layer. DOC decreased sharply from just below the mixed layer to 250 m. The sampling programmes in winter 1992 and 1993 were concurrent with a deep mixing events and mixed layer depths ranged from 160–260 m (Fig. 2b) within which DOC was homogeneously distributed.

The covariance of DOC profiles with the vertical structure of temperature reflects the influence of biological and physical processes, which govern the distribution of DOC. The subsurface maxima observed in the spring and summer DOC profiles indicate an accumulation of DOC due to an uncoupling of production and consumption. In the spring and summer the structure of the DOC profile differed greatly from that of temperature

TABLE 1 A carbon budget for the upper ocean near Bermuda: a comparison of new and export production

Method	Measured parameter (mol m ⁻² yr ⁻¹)	Carbon equivalent (mol C m ⁻² yr ⁻¹)	Ref.
New production			
Oxygen geochemistry	~5 (O ₂)	2.9–4.16*	7
Nitrate flux via ³ He correlation	0.6 (NO ₃)	3.97†	8
Argon, helium, oxygen tracers	5.1 (4.3–5.6) (O ₂)	3.0–4.25*	9
Tritium box model		2.4–3.5	29
Nitrate flux estimated from 18 °C water ventilation	0.38 (NO ₃)	2.5†	27
Export			
Oxygen utilization rate‡	4.1–5.9 (O ₂)	3.3–4.72	7
Sinking PON (100 m sediment traps)	0.2 (PON)	1.32	4
Sinking POC§ (150 m sediment traps)	0.77–0.78 (POC)	0.77–0.78	5
Sinking POC§ (150 m sediment traps)	0.71 (POC)	0.71	6
Advected DOC	0.99–1.21 (DOC)	0.99–1.21	This study

Abbreviations used: PON, particulate organic nitrogen; POC, particulate organic carbon.

* Photosynthetic quotients ranging from 1.2–1.7 were used to calculate annual C production from O.

† C/N ratio of 6.63 was used to estimate annual C production from nitrate flux.

‡ O utilization rates integrated from 100–400 m were used to estimate the total C utilized below the euphotic zone. This value represents a total export of organic material out of the euphotic zone. A respiratory quotient of 0.8 was used to calculate the C utilization from O consumption.

§ Sediment traps were deployed at 150 m. Based on the ocean composite relationship of Martin and colleagues³⁰, one would expect the flux at 150 m to be comparable to 67% of 100 m flux yields.

in the surface 100 m suggesting that biogeochemical rather than physical processes regulated DOC distribution during these seasons. But there was a slight salinity maximum near 50 m in the summer and we cannot rule out the possibility that horizontal advection influenced the profiles. In the autumn and winter, the deepening of the surface mixed layers eradicated the DOC subsurface maximum. DOC appeared to behave conservatively during these seasons with physical mixing processes governing its distribution in the top 250 m.

The relative increases in DOC stocks (\int DOC) within the surface 250 m during March 1991 and 1992 were coincident with phytoplankton blooms (Fig. 2a), indicating that DOC production was greater than consumption during these periods. Despite this production and accumulation, \int DOC in the surface 100 m decreased compared to autumn concentrations (Fig. 2b). As a result of deep mixing, low DOC water was entrained into the

upper 100 m lowering the \int DOC in this layer (Fig. 2b) and higher surface DOC was mixed below the euphotic zone elevating \int DOC in the 100–250 m layer (Fig. 2c). Upon restratification of the water column in April 1992, there was further accumulation of 'freshly produced' DOC in the surface 100 m which increased \int DOC (Fig. 2b) and produced a subsurface maximum (Fig. 1a). We observed a significant decrease ($P < 0.05$) in \int DOC in the upper 100 m from April 1992 to March 1993 (Fig. 2b). From April to November 1992, the surface mixed layer remained well above 100 m eliminating the possibility of DOC removal by deep mixing; we attribute the observed decrease to biological consumption. Approximately $0.5 \text{ mol DOC m}^{-2}$ were consumed at a rate of $\sim 2.3 \text{ mmol C m}^{-2} \text{ d}^{-1}$ in the top 100 m from April to November 1992. The decrease in \int DOC observed from October 1991 to March 1992 and November 1992 to March 1993 (Fig. 2b) was due to dilution of high DOC water by the

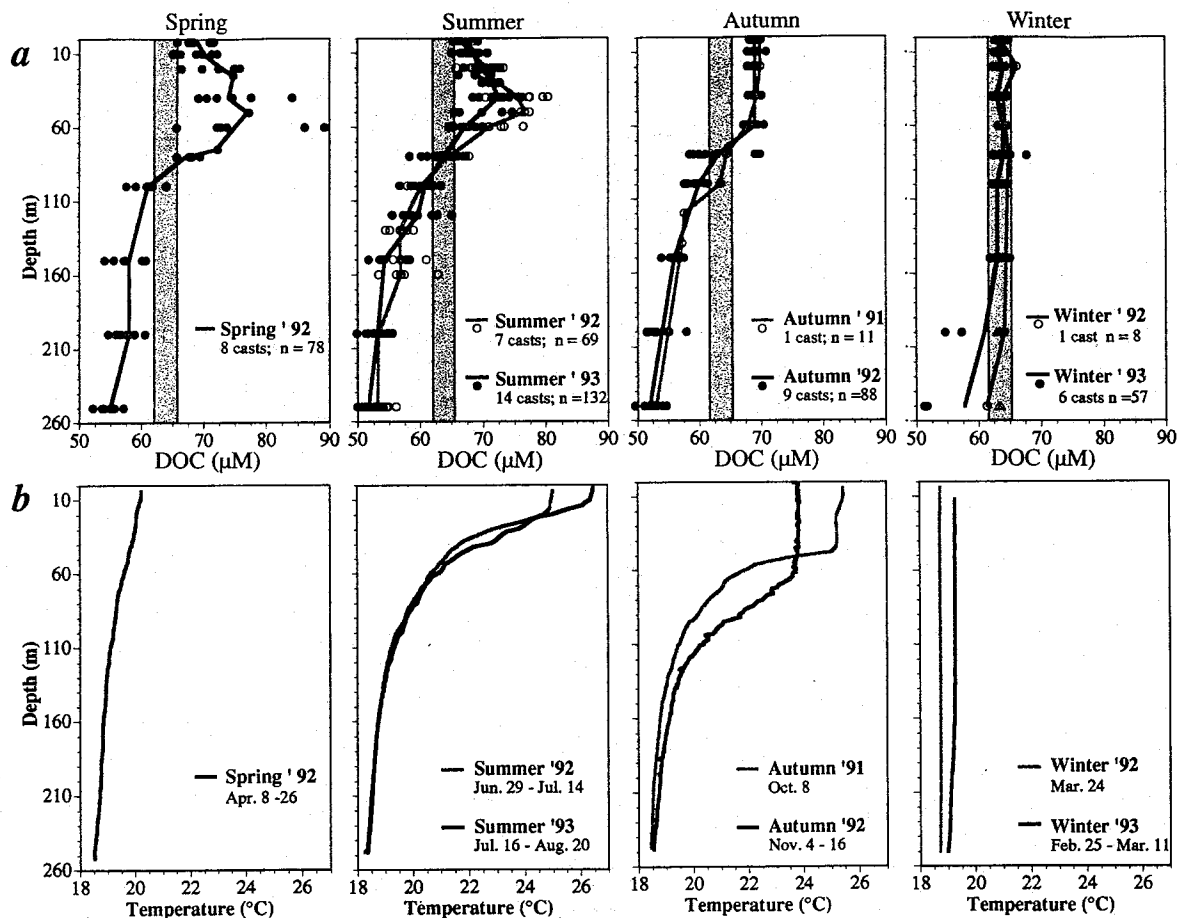


FIG. 1 a, Filled and empty circles are DOC measurements made in the western Sargasso Sea in the vicinity of BATS site ($31^{\circ} 50' \text{ N}$, $64^{\circ} 10' \text{ W}$) and Hydrostation S ($32^{\circ} 10' \text{ N}$, $64^{\circ} 10' \text{ N}$). The lines represent the average profile per season. In winter 1993, the mixed layer extended to 260 m for three casts but samples were only taken in the top 150 m. In all the data we have collected to date, the DOC concentrations were always homogeneously distributed throughout the mixed layer. We assumed this to be true in the three casts in which the whole mixed layer was not sampled. Triangles represent an average of all DOC values within the top 150 m for a given cast and then extended to the base of that cast's mixed layer. In order to emphasize the seasonal dynamics a grey highlighted bar, representing the general range of DOC during winter deep mixing, is shown in each panel. The number of casts and samples (n) collected within a given season are shown in each panel. b, Each panel represents the mean vertical profile of temperature of a given season and year. The dates of the sampling programme are shown in each panel.

METHODS. Niskin bottles were used to collect 10–12 samples per cast within the top 250 m of the water column. The sampling method followed the JGOFS DOC protocol as described previously³¹. Samples were drawn directly from Niskin bottles into precombusted 40-ml vials and sealed with Teflon-coated septa and open top screw caps. Samples were frozen immediately and stored at -20°C until back on land. Before analysis samples were thawed, acidified with 85% H_3PO_4 (30 μl per 30 ml) and sparged with CO_2 -free oxygen at a flow rate of 200 ml min^{-1} for at least 10 min. Samples were analysed by the high temperature combustion technique using a modified Dohrmann DC-190. Operating parameters of the Dohrmann DC-190 were as described previously³¹. All samples were blank-corrected. Analysis was standardized with a 4 point curve of glucose solution in Milli-Q water. Temperature data was collected and processed by Seabird CTD and software for the spring 1992, summer 1992 and winter 1993. Neil Brown CTD was used in the autumn of 1992.

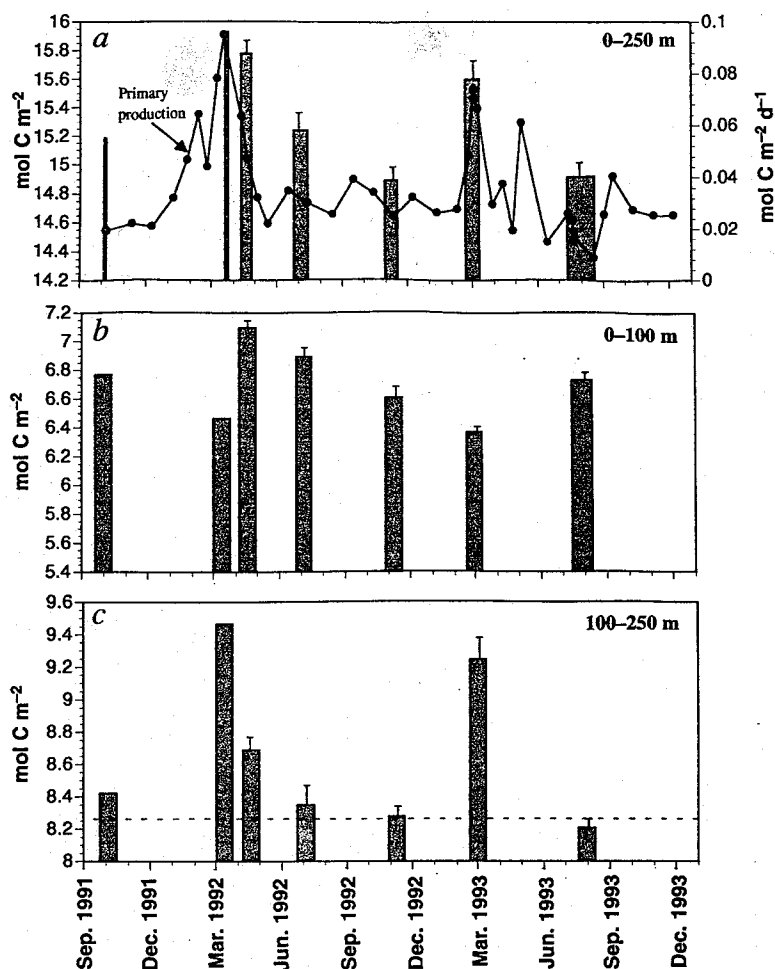


Fig. 2 a, Integrated DOC concentrations and sampling programme (grey bars) compared with the annual pattern of primary production (filled circles). Integrated primary production was estimated by whole day *in situ* ¹⁴C incubations in the top 140 m at the BATS site (31° 50' N, 64° 10' W). The width of the bars represents the length of the DOC sampling period. The height of the bars represents integrated DOC concentration in the surface 250 m. The bars in b and c correspond to the average integrated DOC concentration within the 0-100 m and 100-250 m layers respectively. The error bars are for standard error. The broken line in c represents the background integrated DOC value for the 100-250 m layer (see text).

entrainment of low carbon water into the euphotic zone and not by biological consumption alone.

The \int DOC in the 100-250 m layer increased significantly in both March 1992 and 1993 (Fig. 2c) as a result of entrainment of 'freshly produced' bloom DOC and 'residual' surface DOC. To determine the flux of DOC into the lower layer, we estimated a baseline value of 8.25 mol C m⁻² by calculating the mean of all \int DOC within the 100-250 m layer for autumn 1991, autumn 1992 and summer of 1993 (Fig. 2c). Convection and bloom events resulted in a flux of \sim 1.21 mol DOC m⁻² and 0.99 mol DOC m⁻² into the 100-250 m layer in 1992 and 1993 respectively. These flux estimates are approximately 23-42% of Jenkins and co-workers new production estimates, which are equivalent or greater than the estimated annual sinking flux estimates of particulate organic carbon (POC) in waters near Bermuda (Table 1). Upon restratification, the subsurface DOC was trapped, effectively removing it from the euphotic zone. The significant decrease in 100-250 m \int DOC indicates a subsequent remineralization of this DOC from winter to autumn. Some portion of the exported DOC pool is remineralized rapidly (Fig. 2c; March to April) while another portion representing a semilabile component is mineralized more slowly.

Effective decoupling of DOC production from consumption results in net production in the upper 100 m in spring, and export of DOC escaping mineralization the following winter. This 'residual' pool is comprised of semilabile material left over from the previous year's blooms plus biologically refractory material which has an average age of 4,100 yr (ref. 25). In addition to 'residual' DOC, deep mixing events also export a 'freshly produced' pool. Episodic deep mixing interrupted by short-lived periods of stratification result in production and accumulation

of 'freshly produced' DOC. Upon further deep mixing, as observed in March 1992 and 1993 (Fig. 1), 'freshly produced' DOC, and surface residual DOC are mixed into the 100-250 m layer.

By calculating homogeneous vertical profiles with the same integrated amounts, we determined the potential \int DOC concentration in each layer resulting from deep mixing. These estimates reflect the residual concentrations resulting from physical mixing in which surface layer DOC was diluted and the deeper layer was enriched. For example, if the 15.2 mol C m⁻² in autumn 1991 was redistributed homogeneously over 250 m, then the 0-100 m layer would decrease from 6.8 to 6.1 mol C m⁻² and the 100-250 m layer would increase from 8.4 to 9.1 mol C m⁻². We measured higher values of 6.5 and 9.5 mol C m⁻² for March 1992 (Fig. 2b, c). We attribute this increase to the production, accumulation and distribution of 'freshly produced' DOC. By comparing the estimated residual \int DOC in autumn 1991 and 1992 to actual values from March 1992 and 1993 we estimate conservatively that the exported DOC comprised \sim 32% 'freshly produced' bloom DOC and \sim 67% 'residual' DOC. Thus, a significant portion of the surface DOC pool was removed from the euphotic zone nearly 1 year after its production.

Our results confirm previous evidence of seasonal DOC changes in marine systems^{10,26} and show a clear seasonal pattern of DOC concentrations and distribution in the surface 250 m of the open ocean. In the northwestern Sargasso Sea, deep mixing events which occur in late February-early March, ventilate nutrient-rich water into the euphotic zone^{6,23,27}. The introduction of these nutrients stimulates a phytoplankton bloom which increases concentrations of particulate and dissolved organic material. Convection mixes DOC-enhanced water below the

euphotic zone. The magnitude and depth of this DOC flux and the size of the seasonal accumulation probably depend on the intensity of the deep mixing event. This export is a mixture of locally produced DOC, DOC produced from the previous spring and refractory DOC. Spring stratification effectively sequesters this organic carbon below the euphotic zone, resulting in net remineralization of DOC within the deep surface layer. Consumption of DOC in this layer suggests that this export is not long-term C storage. Oxygen utilization rates integrated between 100–400 m are an independent estimate of the remineralization of new production⁷ and these agree well with the biogeochemical tracer techniques for determining the total new production near Bermuda (Table 1). However, there are large discrepancies between direct measurements of annual POC flux and the annual export inferred from the geochemical tracers. Michaels and colleagues²⁸ have suggested that sediment traps undersample the sinking particulate flux at the BATS site and this bias could explain a significant portion of this discrepancy. Our data indicate that 23–42% of this discrepancy can be explained by convective mixing of DOC. □

Received 2 June; accepted 23 August 1994.

1. Sarmiento, J. L. & Siegenthaler, U. in *Primary Productivity and Biogeochemical Cycles in the Sea* (eds Falkowski, P. G. & Woodhead, A. D.) 317–332 (Plenum, New York, 1992).
2. McCave, I. N. *Deep-Sea Res.* **22**, 491–502 (1975).
3. Eppley, R. W. & Peterson, B. J. *Nature* **282**, 677–680 (1979).
4. Altabet, M. A. *J. geophys. Res.* **94**, 12771–12779 (1989).

5. Lohrenz, S. E. et al. *Deep-Sea Res.* **39**, 1373–1391 (1992).
6. Michaels, A. F. et al. *Deep-Sea Res.* **41**, 1013–1038 (1994).
7. Jenkins, W. J. & Goldman, J. C. *J. Mar. Res.* **43**, 465–491 (1985).
8. Jenkins, W. J. *Nature* **331**, 521–523 (1988).
9. Spitzer, W. S. & Jenkins, W. J. *J. mar. Res.* **47**, 169–196 (1989).
10. Copin-Montégut, G. & Avril, B. *Deep-Sea Res.* **40**, 1963–1972 (1993).
11. Toggweiler, J. R. in *Productivity of the Ocean: Present and Past* (eds Berger, W. H., Smetacek, V. S. & Wefer, G.) 65–83 (Wiley, Dahlem Konferenzen, Germany, 1989).
12. Bacastow, R. & Maier-Reimer, E. *Globl Biogeochem. Cycles* **5**, 71–85 (1991).
13. Majjar, R. G., Sarmiento, J. L. & Toggweiler, J. R. *Globl Biogeochem. Cycles* **6**, 45–76 (1992).
14. Suzuki, Y., Sugimura, Y. & Itoh, T. *Mar. Chem.* **16**, 83–97 (1985).
15. Goldman, J. C., Hansell, D. A. & Dennett, M. R. *Mar. Ecol. Prog. Ser.* **88**, 257–270 (1992).
16. Sugimura, Y. & Suzuki, Y. *Mar. Chem.* **24**, 105–131 (1988).
17. Suzuki, Y. *Mar. Chem.* **41**, 287–288 (1993).
18. Sharp, J. H. et al. *Limnol. Oceanogr.* **38**, 1774–1782 (1993).
19. Hansell, D. A., Williams, P. M. & Ward, B. B. *Deep Sea Res.* **40**, 219–234 (1993).
20. Sharp, J. H. et al. *Mar. Chem.* (in the press).
21. Peltzer, E. T. & Brewer, P. G. *Mar. Chem.* **41**, 243–252 (1993).
22. Benner, R. & Strom, M. *Mar. Chem.* **41**, 153–160 (1993).
23. Menzel, D. W. & Ryther, J. H. *Deep-Sea Res.* **6**, 351–367 (1960).
24. Malone, T. C., Pike, S. E. & Conley, D. J. *Deep-Sea Res.* **40**, 903–924 (1993).
25. Bauer, J. E., Williams, P. M. & Druffel, E. R. M. *Nature* **357**, 667–670 (1992).
26. Duursma, E. K. *Neth. J. Sea Res.* **1**, 1–148 (1961).
27. Siegel, D. A. et al. *J. mar. Res.* **48**, 379–412 (1990).
28. Michaels, A., Buesseler, K., Bates, N., Carlson, C. A. & Knapp, A. *Nature* (submitted).
29. Sarmiento, J. L., Thiele, G., Key, R. M. & Moore, W. S. *J. geophys. Res.* **95**, 18303–18315 (1990).
30. Martin, J. H., Knauer, G. A., Karl, D. M. & Broenkow, W. W. *Deep-Sea Res.* **34**, 127–143 (1987).
31. Carlson, C. A. & Ducklow, H. W. *Deep-Sea Res.* (in the press).

ACKNOWLEDGEMENTS. We thank A. Bryant, J. Cornwell, R. Cuhel, J. Goldman, B. Jenkins, T. Malone, M. Roman, J. Sharp and H. Quinby for discussion and comments on the manuscript and D. Kirchman and R. Toggweiler for constructive comments and reviews. Technical discussions with E. Peltzer improved our analytical techniques. We thank the BATS technicians for logistical and sampling assistance. This research was supported by NSF and the JGOF program.

Increased pressure from rising bubbles as a mechanism for remotely triggered seismicity

Alan T. Linde*, I. Selwyn Sacks*, Malcolm J. S. Johnston†, David P. Hill† & Roger G. Bilham‡

* Department of Terrestrial Magnetism, Carnegie Institution of Washington, 5241 Broad Branch Road NW, Washington DC 20015, USA

† US Geological Survey, 345 Middlefield Road, Menlo Park, California 94025, USA

‡ Department of Geological Sciences, University of Colorado, Boulder, Colorado 80309-0216, USA

AFTERSHOCKS of large earthquakes tend to occur close to the main rupture zone, and can be used to constrain its dimensions. But following the 1992 Landers earthquake (magnitude $M_w = 7.3$) in southern California, many aftershocks were reported¹ in areas remote from the mainshock. Intriguingly, this remote seismicity occurred in small clusters near active volcanic and geothermal systems. For one of these clusters (Long Valley, about 400 km from the Landers earthquake), crustal deformation associated with the seismic activity was also monitored. Here we argue that advective overpressure^{2–7} provides a viable mechanism for remote seismicity triggered by the Landers earthquake. Both the deformation and seismicity data are consistent with pressure increases owing to gas bubbles rising slowly within a volume of magma. These bubbles may have been shaken loose during the passage of seismic waves generated by the mainshock.

Hill *et al.*¹ describe the seismicity following the Landers earthquake in southern California on 28 June 1992 and show that seismicity levels were higher in a number of regions (all with volcanic history) remote from the Landers mainshock. One is the Long Valley caldera, which has a variety of instrumentation in place because of continuing concern about a possible

eruption⁸. Langbein *et al.*⁸ model ground surface motions during 1989–91 in terms of increased pressure in a spherical source at 7-km depth under the resurgent dome together with growth of a dyke (vertical magma-filled opening) under Mammoth Mountain. These changes resulted in increased seismicity, although the spatial distribution suggests a more complex geometry than in the simple model. Figure 1 shows maps of the Long Valley caldera comparing the seismicity in the 5 days before the Landers earthquake with that in the 5 days after it. Also shown are the sites of a Sacks–Evertson borehole strainmeter⁹ (POP), a long-baseline tiltmeter¹⁰ (LBT) and the proposed pressure sources of Langbein *et al.*⁸. The triggered seismicity has an areal distribution, and magnitudes and depths, similar to those of earthquakes occurring usually in this region¹. The obvious inference is that the triggered seismicity is due to the same process that drives the continuing seismicity, except that after the Landers earthquake the process was enhanced.

Figure 2 shows the cumulative seismicity at Long Valley together with the dilatation at POP and the east–west tilt at LBT (similar plots of seismicity and dilatation were shown in Hill *et al.*¹). We see the clear correlation between the rapid increase in the cumulative number of earthquakes over about 4 or 5 days and the increase in contraction at POP as well as the change in tilt at LBT. Suggested mechanisms for the remote triggered seismicity include hydraulic pumping of high-pressure pore fluids¹, relaxation of partially crystallized magma bodies¹, enhancement by fault connectivity of static strain¹¹ and aseismic slip triggered by dynamic strain^{12,13}. None of these suggested mechanisms can adequately explain either the duration of the triggered activity or the form of the deformation transient. Here, as it seems clear that the continuing seismicity results from increased pressure in magma under Long Valley, we look for an explanation of the triggered seismicity in terms of a process which increases that pressure, resulting in the observed deformations and the increase in seismicity.

We consider the advective overpressure mechanism^{2–5} as a viable candidate. Our attention was drawn to this by Sahagian and Proussevitch^{6,7}, who showed that if a bubble of perfect gas rises in an incompressible liquid inside a rigid sealed container,